Langmuir
Article
pubs.acs.org/Langmuir

Highly Controlled Silica Coating of PEG-Capped Metal Nanoparticles and Preparation of SERS-Encoded Particles†

Cristina Fernández-López, Cintia Mateo-Mateo, Ramón A. Álvarez-Puebla, Jorge Pérez-Juste, Isabel Pastoriza-Santos,* and Luis M. Liz-Marzán*

Departamento de Química Física and Unidad Asociada CSIC-Universidade de Vigo, 36310 Vigo, Spain

Received May 8, 2009. Revised Manuscript Received June 16, 2009

Thiol-modified poly(ethylene glycol) (mPEG-SH) has been used to replace standard capping agents from the surfaces of gold nanoparticles with different sizes and shapes. Upon PEG stabilization, the nanoparticles can be transferred into ethanol, where silica can be directly grown on the particle surfaces through the standard Stöber process. The obtained silica shells are uniform and homogeneous, and the method allows a high degree of control over shell thickness for any particle size and shape. Additionally, Raman-active molecules can be readily incorporated within the composite nanoparticles during silica growth so that SERS/SERRS-encoded nanoparticles can be fabricated containing a variety of tags, thereby envisaging multiplexing capability.

Introduction

The development of new strategies for coating metal nanoparticles with silica has been an important issue during the last 15 years.[1−10] This research has been nourished by the numerous possibilities that silica coating offers in many fields of materials and biomaterials science, but it shows in almost all cases the limitation of being specific to a particular type of nanoparticle or surface capping agent.[1,2,5] Whereas initially silica was reported as an ideal coating material to enhance the colloidal stability of nanoparticles, provide tunable solubility in various solvents, or even tailor their size and shape-dependent optical properties,[1,6,11−13] its easy functionalization has opened up a wide range of new expectations in biomedical applications, for example, as sensors, markers, and probes.[5,14−16] In particular, encoded nanoparticles[17] have gained prominence as a fast, reliable, and sensitive tool not only for multiplexed high-throughput screening,[18,19] biodiagnosis,[20] and bioimaging[21−23] but also for the encoding/identification of commercial goods, documents (i.e., passports or ID cards), and bank notes. Regarding the fabrication of encoded particles,[24] several alternatives have been reported for the unique introduction of the code into each batch of single particles. For example, particles have been internally labeled through shape,[25] composition,[26] or lithographic marks.[27] However, particles may also be externally labeled by introducing quantum dots,[28−32] fluorescent dyes,[33,34] or Raman molecular codes[35−37] into their structures. Along these lines, the introduction of surface-enhanced Raman reporters into hybrid particles composed of plasmonic nanostructures such as gold nanoparticles[36] or connected islands[38] and silica coating shells can expedite

† Part of the "Langmuir 25th Year: Nanoparticles synthesis, properties, and assemblies" special issue.

*Fax: +34 986812556. E-mail: pastoriza@uvigo.es; lmarzan@uvigo.es.

(1) Liz-Marzán, L. M.; Giersig, M.; Mulvaney, P. *Langmuir* **1996**, *12*, 4329.
(2) Obare, S. O.; Jana, N. R.; Murphy, C. J. *Nano Lett.* **2001**, *1*, 601.
(3) Mine, E.; Yamada, A.; Kobayashi, Y.; Konno, M.; Liz-Marzán, L. M. *J. Colloid Interface Sci.* **2003**, *264*, 385.
(4) Graf, C.; Vossen, D. L. J.; Imhof, A.; van Blaaderen, A. *Langmuir* **2003**, *19*, 6693.
(5) Liu, S.; Hang, M. *Adv. Funct. Mater.* **2005**, *15*, 961.
(6) Shen, R.; Camargo, P. H.; Xia, Y.; Yang, H. *Langmuir* **2009**, *24*, 11189.
(7) Pastoriza-Santos, I.; Pérez-Juste, J.; Liz-Marzán, L. M. *Chem. Mater.* **2006**, *18*, 2465.
(8) Han, Y.; Jiang, J.; Lee, S. S.; Ying, J. Y. *Langmuir* **2008**, *24*, 5842.
(9) Gorelikov, I.; Matsuura, N. *Nano Lett.* **2008**, *8*, 369.
(10) Lee, D. C.; Mikulec, F. V.; Pelaez, J. M.; Koo, B.; Korgel, B. A. *J. Phys. Chem. B* **2006**, *110*, 11160.
(11) Pastoriza-Santos, I.; Sánchez−Iglesias, A.; García de Abajo, F. J.; Liz-Marzán, L. M. *Adv. Funct. Mater.* **2007**, *17*, 1443.
(12) Rodríguez-Fernández, J.; Pastoriza-Santos, I.; Pérez-Juste, J.; Liz-Marzán, L. M. *J. Phys. Chem. C* **2007**, *111*, 13361.
(13) Ung, T.; Liz-Marzán, L. M.; Mulvaney, P. *J. Phys. Chem. B* **2001**, *105*, 3441.
(14) Sha, M. Y.; Xu, H.; Natan, M. J.; Cromer, R. *J. Am. Chem. Soc.* **2009**, *130*, 17214.
(15) Wang, C.; Ma, Z.; Wang, T.; Su, Z. *Adv. Funct. Mater.* **2006**, *16*, 1673.
(16) Küstner, B.; Gellner, M.; Schütz, M.; Schöppler, F.; Marx, A.; Ströbel, P.; Adam, P.; Schmuck, C.; Schlücker, S. *Angew. Chem., Int. Ed.* **2009**, *48*, 1950.
(17) Braeckmans, K.; De Smedt, S. C.; Leblans, M.; Roelant, C.; Demeester, J. *Nat. Rev. Drug. Discovery* **2002**, *1*, 1.
(18) Doerr, A. *Nat. Methods* **2007**, *4*, 381.
(19) Fenniri, H.; Alvarez-Puebla, R. *Nat. Chem. Biol.* **2007**, *3*, 247.
(20) Zhao, Y. J.; Zhao, X. W.; Hu, J.; Xu, M.; Zhao, W. J.; Sun, L. G.; Zhu, C.; Xu, H.; Gu, Z. Z. *Adv. Mater.* **2009**, *21*, 569.
(21) Howarth, M.; Liu, W. H.; Puthenveetil, S.; Zheng, Y.; Marshall, L. F.; Schmidt, M. M.; Wittrup, K. D.; Bawendi, M. G.; Ting, A. Y. *Nat. Methods* **2008**, *5*, 397.
(22) Serge, A.; Bertaux, N.; Rigneault, H.; Marguet, D. *Nat. Methods* **2008**, *5*, 687.
(23) Qian, X.; Peng, X.-H.; Ansari, D. O.; Yin-Goen, Q.; Chen, G. Z.; Shin, D. M.; Yang, L.; Young, A. N.; Wang, M. D.; Nie, S. *Nat. Biotechnol.* **2008**, *26*, 83–90.
(24) Nam, J. M.; Park, S. J.; Mirkin, C. A. *J. Am. Chem. Soc.* **2002**, *124*, 3820–3821.
(25) Vaino, A. R.; Janda, K. D. *Proc. Natl. Acad. Sci. U.S.A.* **2000**, *97*, 7692.
(26) Raez, J.; Blais, D. R.; Zhang, Y.; Alvarez-Puebla, R. A.; Bravo-Vasquez, J. P.; Pezacki, J. P.; Fenniri, H. *Langmuir* **2007**, *23*, 6482.
(27) Pregibon, D. C.; Toner, M.; Doyle, P. S. *Science* **2007**, *315*, 1393.
(28) Derveaux, S.; De Geest, B. G.; Roelant, C.; Braeckmans, K.; Demeester, J.; De Smedt, S. C. *Langmuir* **2007**, *23*, 10272.
(29) Han, M. Y.; Gao, X. H.; Su, J. Z.; Nie, S. *Nat. Biotechnol.* **2001**, *19*, 631.
(30) Bruchez, M.; Moronne, M.; Gin, P.; Weiss, S.; Alivisatos, A. P. *Science* **1998**, *281*, 2013.
(31) Nicewarner-Pena, S. R.; Freeman, R. G.; Reiss, B. D.; He, L.; Pena, D. J.; Walton, I. D.; Cromer, R.; Keating, C. D.; Natan, M. J. *Science* **2001**, *294*, 137.
(32) Cunin, F.; Schmedake, T. A.; Link, J. R.; Li, Y. Y.; Koh, J.; Bhatia, S. N.; Sailor, M. J. *Nat. Mater.* **2002**, *1*, 39.
(33) Johnston, A. P. R.; Battersby, B. J.; Lawrie, G. A.; Lambert, L. K.; Trau, M. *Chem. Mater.* **2006**, *18*, 6163.
(34) Stoermer, R. L.; Keating, C. D. *J. Am. Chem. Soc.* **2006**, *128*, 13243.
(35) Sha, M. Y.; Xu, H.; Natan, M. J.; Cromer, R. *J. Am. Chem. Soc.* **2008**, *130*, 17214.
(36) Doering, W. E.; Piotti, M. E.; Natan, M. J.; Freeman, R. G. *Adv. Mater.* **2007**, *19*, 3100.
(37) Qin, L.; Banholzer, M. J.; Millstone, J. E.; Mirkin, C. A. *Nano Lett.* **2007**, *7*, 3849.
(38) Sanles-Sobrido, M.; Exner, W.; Rodríguez-Lorenzo, L.; Rodríguez-González, B.; Correa-Duarte, M. A.; Álvarez-Puebla, R. A.; Liz-Marzán, L. M. *J. Am. Chem. Soc.* **2009**, *131*, 2699.

the read-out process while preserving the Raman reporter from leaching or contamination and can provide a versatile surface for functionalization.

The successful growth of uniform silica shells on metal nanoparticles has long been hindered by the low chemical affinity between both components. Therefore, most of the reported silica coating routes are based on priming the metal surface with coupling agents, surfactants, or polymers.[1,2,6,7,9,39] The role of such surface priming is not just to increase the affinity of the metallic surface toward silica but also to provide the colloids with sufficient stability to be transferred into ethanol or isopropanol so that the classical Stöber method[40] can be used for the growth of uniform silica shells on the metallic cores. Liz-Marzán et al.[1] first reported a method for coating citrate-stabilized gold nanoparticles with silica by using a silane coupling agent to induce the formation of a thin silica shell by sodium silicate (active silica) condensation prior to solvent exchange and subsequent growth by means of the Stöber method. Graf et al.[4] developed a more general method based on the use of poly(vinylpyrrolidone) (PVP) as a primer because this polymer can adsorb onto a wide range of different materials (metals, metal oxides, silica, polystyrene, etc.) and direct the growth of silica on the particle surface by the addition of tetraethoxysilane (TEOS) to an ammonia−ethanol solution. Although the PVP-assisted silica coating failed for cetyltrimethylammonium bromide (CTAB)-stabilized nanoparticles, Pastoriza-Santos et al.[7] circumvented this problem by wrapping gold nanorods with polyelectrolyte layers prior to PVP coating. Although the polymer-based approach leads to homogeneous coatings, proper choice of the polymer molecular weight proved to be critical. More recently, Shen et al.[6] also used a silane coupling agent (methoxy-poly(ethylene glycol) silane) to transfer nanoparticles from hydrophobic to hydrophilic solvents, thereby enabling the growth of SiO_2 onto the particle surfaces. Gorelikov et al.[9] reported the direct silica coating of CTAB-capped gold nanoparticles with no need for a priming step, leading to the formation of rather thick mesoporous silica shells because of the templating effect of CTAB on which TEOS can hydrolyze, thereby promoting silica condensation. Alternatively, the growth of silica shells can also be achieved by incorporating preformed nanoparticles within microemulsion droplets without the use of any specific coupling agent or polymer to enhance the surface affinity.[5,8] This was used by Han et al.[8] to coat oleylamine-stabilized gold and silver nanoparticles (<20 nm) with good control over shell thickness. In this case, the polyoxyethylene(5)-nonylphenyl ether (Igepal CO-520) used as a surfactant contains several ether groups that could strongly interact with silanes through hydrogen bonding, thus generating preferred sites for silica nucleation and growth.[41−43]

We present in this article a rapid, simple strategy that can be applied to coat gold nanoparticles with a variety of shapes, as demonstrated for spheres (in a wide size range) and nanorods with homogeneous silica shells, and which allows a high degree of control over shell thickness. This method involves using methoxy-poly(ethylene glycol)-thiol (mPEG-SH) as a coupling agent to transfer the particles into ethanol, where silica can be directly grown on the particle surfaces through the standard Stöber process. Additionally, we demonstrate that the incorporation of Raman-active molecules during silica growth is straightforward, thus simplifying the fabrication of SERS-encoded nanoparticles.

Experimental Section

Chemicals. Tetrachloroauric acid ($HAuCl_4 \cdot 3H_2O$), tetraethylorthosilicate (TEOS), NH_4OH (29%), and Nile blue A (NBA) perchlorate were purchased from Aldrich. Ascorbic acid, sodium citrate ($C_6H_5O_7Na_3 \cdot 2H_2O$), silver nitrate ($AgNO_3$), sodium borohydride ($NaBH_4$), methylene blue (MB), and toluidine blue O (TB) were supplied by Sigma. Cetyltrimethylammonium bromide (CTAB) and *O*-[2-(3-mercaptopropionylamino)ethyl]-*O*′-methyl-poly(ethylene glycol) (mPEG-SH, M_w 5000) were procured from Fluka. HCl (37%) was supplied by Panreac. All chemicals were used as received. Pure-grade ethanol and Milli-Q-grade water were used in all preparations.

Gold Nanosphere Synthesis. Citrate-stabilized Au nanospheres ($d = 15.5 \pm 2.1$ nm, [Au] = 0.5 mM) were synthesized as reported by Turkevich.[44] CTAB-stabilized gold nanospheres with various sizes (60.4 ± 3.4, 98.5 ± 7.0, and 142.8 ± 8.1 nm) were prepared by seeded growth as previously described.[45] The first growth step was carried out by the addition of ascorbic acid (0.5 mM) to a solution containing $HAuCl_4$ (0.25 mM) and 0.015 M CTAB at 35 °C, followed by the addition of the seed solution (15 nm citrate-Au seeds in a final concentration of $[Au] = 3.97 \times 10^{-6}$ M). Subsequently, nonspherical particles formed during the process were removed through CTAB-assisted shape-selective separation.[46] The resulting gold nanospheres ($d = 60.4 \pm 3.4$ nm, as determined from TEM images) were grown in a similar fashion up to final diameters of 98.5 ± 7 and 142.8 ± 8 nm, as determined from TEM. The Au concentrations of 60.4 nm seeds (after addition to the growth solution) used for growing 98.5 and 142.8 nm particles were 6.89×10^{-5} and 1.71×10^{-5} M, respectively.

Gold Nanorod Synthesis. Gold nanorods were prepared by Ag-assisted seeded growth.[47] The seed solution was prepared by the borohydride reduction of 5 mL of 0.25 mM $HAuCl_4$ in a 0.1 M aqueous CTAB solution. The average particle size measured from TEM was 2.8 ± 0.7 nm. The seed solution (12 or 24 μL) was added to a growth solution containing 0.1 M CTAB, 0.5 mM $HAuCl_4$, 0.019 M HCl, 0.8 mM ascorbic acid, and 0.12 mM silver nitrate. The dimensions of the obtained gold nanorods were 19.0 ± 2.7 nm $\times$ 66.8 ± 7.4 nm and 14.3 ± 2.0 nm $\times$ 67.4 ± 11.2 nm, with aspect ratios of 3.5 ± 0.5 and 4.8 ± 0.7, respectively.

mPEG-SH Capping, Ethanol Transfer, and Silica Coating. An aqueous solution containing 1.36×10^{-7} moles of mPEG-SH (calculated to provide 4 molecules/nm^2), previously sonicated for 15 min, was added dropwise under vigorous stirring to 10 mL of as-synthesized 15.5 nm spheres ([Au] = 0.5 mM). The mixture was allowed to react for 30 min. PEG-modified particles were then centrifuged (3000 rpm, 6 h) twice to remove excess mPEG-SH and redispersed in 2 mL of ethanol, where silica coating was carried out through adjustment of the final concentrations as follows: [Au] = 0.5 mM, $[H_2O] = 10.55$ M, $[NH_3] = 0.2$ M, and [TEOS] = 0.8 mM. The reaction mixture was allowed to react for 2 h, and at this stage, the shell could be grown upon controlled TEOS addition. Prior to each TEOS addition, centrifugation is recommended to remove free silica nuclei.

For CTAB-capped spheres, 20 mL of the as-synthesized (60/98/143 nm) spheres ([Au] = 0.25 mM, [CTAB] = 0.015 M) was centrifuged for 15 min (4000/2500/1500 rpm). The precipitate was collected and redispersed with Milli-Q water to a final volume of 10 mL to obtain [CTAB] ~1 mM and [Au] ~0.5 mM. An aqueous solution containing 4 mPEG-SH molecules/nm^2

(39) Ung, T.; Liz-Marzan, L. M.; Mulvaney, P. *Langmuir* **1998**, *14*, 3740.
(40) Stöber, W.; Fink, A.; Bohn, E. *J. Colloid Interface Sci.* **1968**, *26*, 62.
(41) Boissière, C.; Larbot, A.; Bourgaux, C.; Prouzet, E.; Bunton, C. A. *Chem. Mater.* **2001**, *13*, 3580.
(42) Elimelech, H.; Avnir, D. *Chem. Mater.* **2008**, *20*, 2224.
(43) Tiberg, F.; Brinck, J.; Grant, L. *Curr. Opin. Colloid Interface Sci.* **2000**, *4*, 411.
(44) Enüstün, B. V.; Turkevich, J. *J. Am. Chem. Soc.* **1963**, *85*, 3317.
(45) Rodríguez-Fernández, J.; Pérez-Juste, J.; García de Abajo, F. J.; Liz-Marzán, L. M. *Langmuir* **2006**, *22*, 7007.
(46) Jana, N. R. *Chem. Commun.* **2003**, 1950.
(47) Nikoobakht, B.; El-Sayed, M. A. *Chem. Mater.* **2003**, *15*, 1957.

(3.39×10^{-8} moles for 60 nm particles, 2.07×10^{-8} moles for 98 nm particles, and 1.43×10^{-8} moles for 143 nm particles), previously sonicated for 15 min, was added dropwise under vigorous stirring to the sample and stirred for 30 min. The PEG-modified particles were centrifuged twice to remove excess mPEG-SH and redispersed in ethanol (2 mL). Silica coating was performed as described for 15.5 nm Au particles.

For gold nanorods, excess CTAB was removed from a freshly prepared dispersion (20 mL) by initial centrifugation at 8000 rpm for 20 min, redispersion in 20 mL of Milli-Q water, and subsequent centrifugation (2-fold, 6000 rpm). The precipitate was then redispersed with Milli-Q water to a final volume of 10 mL to obtain [CTAB] ~1 mM and [Au] ~0.7 mM. An aqueous solution containing 5.53×10^{-6} moles of mPEG-SH (150 molecules/nm^2), previously sonicated for 15 min, was added dropwise under vigorous stirring, and the mixture was gently stirred for 3 h. PEG-modified nanorods were centrifuged twice to remove excess mPEG-SH and redispersed in ethanol (2 mL). Silica coating was performed as previously explained for 15.5 nm Au particles.

Encoding of Coated Nanoparticles. The encapsulation of Raman probes was carried out by simply adding the dye (diluted in ethanol) dropwise under gentle stirring to the PEG-stabilized Au colloids immediately prior to TEOS addition. The final concentrations of added dye were 6 μM for Nile blue A, 6 μM for methylene blue, and 3 μM for toluidine blue O.

Characterization. Transmission electron microscopy (TEM) was carried out with a JEOL JEM 1010 transmission electron microscope operating at an acceleration voltage of 100 kV. Size (and thickness) distributions were determined from TEM images using at least 100 particles. Vis−NIR spectra were measured with an Agilent 8453 spectrophotometer. Surface-enhanced resonance Raman scattering (SERRS) and electronic emission were measured with a Renishaw Invia Reflex system equipped with a confocal optical microscope, high-resolution gratings (1800 g mm^{-1}), and a Peltier CCD detector by using excitation laser lines at 633 nm (SERRS) and 532 nm (electronic emission). Spectra were collected by focusing the laser line onto the sample (10 μL of each solution cast on a glass slide for SERRS or the bulk dye for fluorescence) by using a 50× objective (N.A. 0.75), providing a spatial resolution of about 1 μm^2 with an accumulation time of 10 s. The power at the sample was 10 μW for SERRS and 1 mW for fluorescence.

Results and Discussion

Poly(ethylene glycol) (PEG) has become an extremely relevant surface functional group for a variety of nanoparticles because it renders them biocompatible. Apart from exhibiting much lower toxicity,[48−50] PEG-modified particles present remarkable resistance against nonspecific protein adsorption[51] and longer in vivo circulation time in blood,[52] which seems to be related to their resistance to clearance via the reticuloendothelial system (RES). In the present work, we demonstrate that the presence of the PEG functionality on the surfaces of nanoparticles additionally enhances their stability in ethanol, thereby facilitating coating with silica by means of the well-known Stöber method. Because of the low reactivity of gold, mercapto-functionalized PEG (mPEG-SH; M_w 5000) was used for the initial ligand exchange. Thus, 15.5 nm citrate-stabilized spherical gold nanoparticles and CTAB-stabilized spherical (60.5, 98.5, and 142.8 nm) gold nanoparticles were transferred into ethanol upon replacement of the original capping agents (citrate ions and CTAB surfactant bilayers) with mPEG-SH, driven by the stronger interaction of thiol groups with the gold surface. Upon ligand exchange, the Au nanoparticles could be readily transferred from water into ethanol without observing any aggregation as revealed by UV−vis spectroscopy measurements. As shown in Figure S1, the UV−vis spectra of all colloids remained unaltered after solvent transfer, regardless of the initial capping agent and particle size, except for a small red shift of the plasmon band arising from the higher refractive index of ethanol (1.36) as compared to that of water (1.33).[53]

The main role of the initial PEG surface modification is enhancing colloidal stability so that the nanoparticles can be readily dispersed in an ethanol/ammonia mixture without aggregation and silica coating can be carried out through the Stober method. Additionally, as previously described for PVP,[2] PEG can serve as a primer to facilitate the condensation of silica onto the metal surface, which is supported by several reports in the literature regarding the affinity of PEG by silica.[41−43] The silanol groups might bind to PEG through hydrogen bonding via PEG ether oxygens, which act as hydrogen bond acceptors. Therefore, we propose the use of PEG as an alternative way to grow silica shells directly on colloidal nanoparticles.

The amount of mPEG-SH added to the initial Au spherical colloids was adjusted to provide 4 mPEG-SH molecules per nm^2 of Au nanoparticle surface. This value was chosen as a compromise to maintain colloidal stability during solvent transfer (aggregation was found to occur for lower surface coverage) while preventing secondary silica nucleation and branching. After the transfer of PEG-capped Au nanoparticles from water to ethanol, the particles were diluted with a mixture of aqueous ammonia and ethanol, onto which a certain amount of TEOS (dissolved in ethanol) was added. As shown in Figures 1 and S2, regardless of particle size, each single gold nanoparticle was individually coated with a uniform silica shell when the optimized amount of 4 molecules per Au nm^2 was used. It is noteworthy that in the case of 15.5 nm Au nanoparticles, coating with a silica shell as thin as 6.1±2.1 nm was sufficient to render the metal colloids perfectly stable against aggregation.

As previously reported,[1,12] coating gold nanoparticles with silica gives rise to a significant red shift in the corresponding surface plasmon bands (SPBs) as displayed in the vis−NIR spectra plotted in Figure 2. This effect can be easily explained in terms of the higher refractive index of amorphous silica (1.46) as compared to that for ethanol (1.36), which produces a decrease in the restoring force on the electron oscillation associated with the plasmon modes.[53] If we analyze the shift of the dipolar SPBs resulting from the silica coating for different Au core sizes (inset of Figure 2), then we find that it increases as the Au core size is increased, which is justified by the higher sensitivity of larger particles toward local refractive index changes, as previously reported for Au decahedra[54] and Ag nanoprisms.[55] For example, the deposition of 24 nm silica shells produces an SPB shift of ca. 33 nm for 142.8 nm Au particles whereas the shift is only 10 nm for 98.5 nm Au cores and 8 nm for 60.4 nm cores. For 15 nm cores, the shift produced by a similarly thick shell was reported to be 6 nm.[1]

A similar approach was used to coat Au nanorods. Whereas in the past a few techniques were reported to coat CTAB-capped Au nanorods with silica, they all suffered from some drawbacks,

(48) Niidome, T.; Yamagata, M.; Okamoto, Y.; Akiyama, Y.; Takahashi, H.; Kawano, T.; Katayama, Y.; Niidome, Y. *J. Controlled Release* **2006**, *114*, 343.
(49) Ballou, B.; Lagergholm, B. C.; Ernst, L. A.; Bruchez, M. P.; Waggoner, A. S. *Bioconjugate Chem.* **2004**, *15*, 79.
(50) Kirchner, C.; Liedl, T.; Kudera, S.; Pellegrino, T.; Javier, M. A.; Gaub, H. E.; Stlzle, S.; Fertig, N.; Parak, W. J. *Nano Lett.* **2005**, *5*, 331.
(51) Bearinger, J. P.; Terrettaz, S.; Michel, R.; Tirelli, N.; Vogel, H.; Textor, M.; Hubbell, J. A. *Nat. Mater.* **2003**, *2*, 259.
(52) Prencipe, G.; Tabakman, S. M.; Welsher, K.; Liu, Z.; Goodwin, A. P.; Zhang, L.; Henry, J.; Dai, H. *J. Am. Chem. Soc.* **2009**, *131*, 4783.
(53) Mulvaney, P. *Langmuir* **1996**, *12*, 788.
(54) Pastoriza-Santos, I.; Sánchez-Iglesias, A.; García de Abajo, F. J.; Liz-Marzán, L. M. *Adv. Funct. Mater.* **2007**, *17*, 1443.
(55) Pastoriza-Santos, I.; Liz-Marzán, L. M. *Nano Lett.* **2002**, *2*, 903.

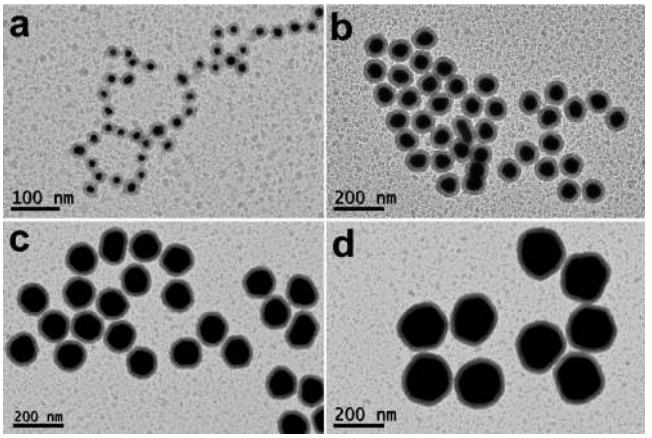

Figure 1. TEM images of Au spherical particles coated with a homogeneous silica shell. (a) 15.5 ± 2.1 nm Au core diameter, 6.1 ± 2.1 nm silica shell thickness. (b) 60.4 ± 3.4 nm Au core diameter, 21.0 ± 2.7 nm silica shell thickness. (c) 98.5 ± 7.0 Au core diameter, 20.9 ± 2.4 nm silica shell thickness. (d) 142.8 ± 8.1 nm Au core diameter, 24.2 ± 3.0 nm silica shell thickness.

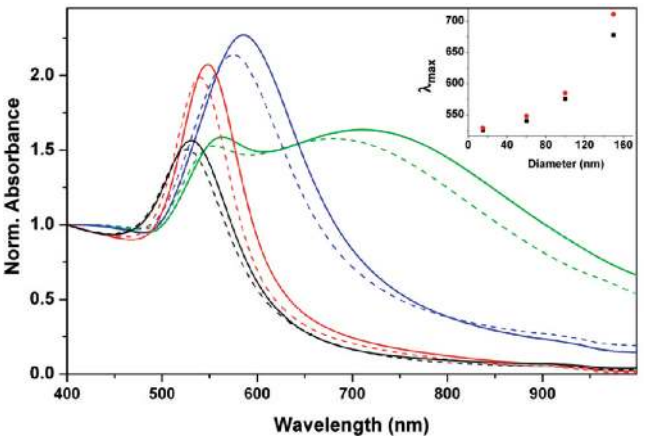

Figure 2. Vis−NIR spectra (---) of PEG-capped Au spheres (in ethanol) of various diameters: 15.5 (black), 60.4 (red), 98.5 (blue), and 142.8 (green) nm. Vis−NIR spectra of the same particles upon silica coating (−). The silica shell thicknesses are 6.1, 21.0, 20.9, and 24.2 nm, respectively. All of the spectra were normalized to 1 at 400 nm to facilitate comparison. (Inset) Plot of the dipolar SPB position of PEG-coated and silica-coated Au nanoparticles vs core diameter.

such as nonuniform or rather thick shells, and only the use of polyelectrolyte multilayers was demonstrated to provide reasonable control over uniformity and shell thickness. In the present method, 4 mPEG-SH molecules/nm^2 again proved sufficient to transfer the CTAB-capped nanorods into ethanol, but when ammonia and TEOS were added, nonhomogeneous silica coating (particles that appeared to be only partially coated) and partial aggregation were observed. In a systematic study, it was found that complete, homogeneous silica shells could be obtained only when a significant excess of mPEG-SH molecules was used, corresponding to 150 molecules/nm^2. This might be related to the denser structure of the CTAB bilayer at the sides of nanorods, as compared to spheres (with much higher curvature), so that a larger number of mPEG-SH molecules are required to replace it. Figure 3a clearly shows the uniformity of the obtained silica shells grown on Au nanorods (66.8 ± 7.4 nm long, 19.0 ± 2.7 nm thick), with a shell thickness of 29.4 ± 2.7 nm. The effect of such silica shells on the optical response of these particles is displayed in

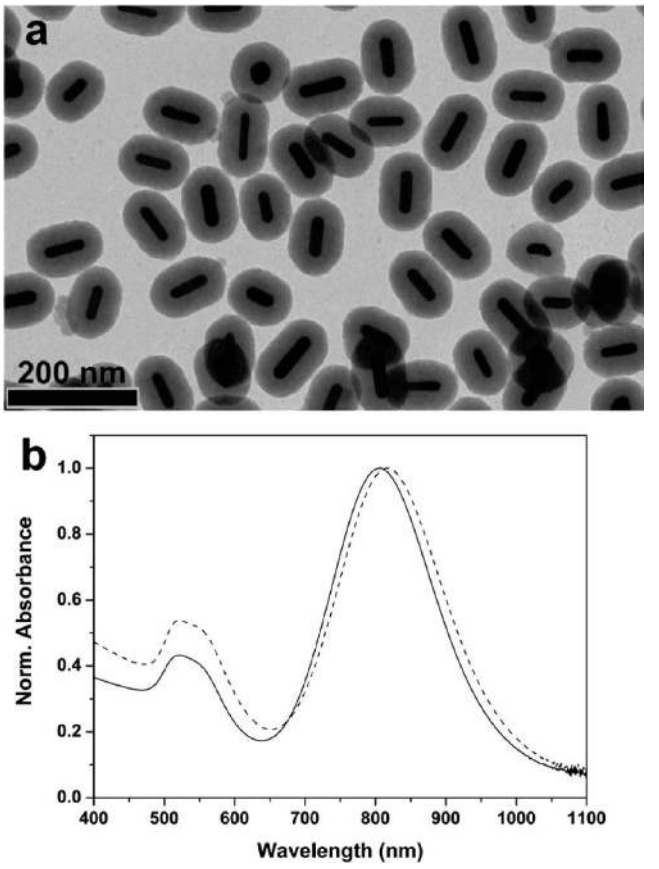

Figure 3. (a) TEM image of silica-coated Au nanorods. (b) Vis−NIR spectra of Au(rods)@PEG colloids before (−) and after (---) silica coating. The spectra were normalized at the longitudinal SPB maximum.

Figure 3b. Whereas the longitudinal surface plasmon (LSP) band was found to red shift by as much as 15 nm (from 805 to 820 nm) because of the local refractive index increase, the transverse plasmon band remains basically unaltered at 525 nm. This result agrees with previous reports[7] and with the higher sensitivity of Au nanorods as compared to spheres,[56] since the 60.4 nm Au spheres (with a larger volume) the band was shifted by only 8 nm when a silica shell of similar thickness was deposited. Additionally, we also observe that the absorbance at wavelengths below 650 nm clearly increases as a result of the stronger (Rayleigh) light scattering arising from the larger particles after silica coating. The observed optical effects clearly confirm that there has been absolutely no aggregation during silica coating.

An advantage of this method over previously reported ones is that it readily provides fine control over the thickness of the silica shells, even for rather thin shells, by simply varying the amount of TEOS added for the initial coating as well as for subsequent additions used for seeded growth. This is clearly demonstrated by the TEM images in Figures 4 and 5 for the multistep silica coating of 60.4 nm Au spheres and 67.4 ×14.3 nm Au nanorods. Such fine control over the shell thickness can be extremely useful for a number of applications that have been hindered by the various difficulties encountered in previously reported procedures.

So far, we have described a general strategy to coat spherical and rod-shaped gold nanoparticles of arbitrary size with uniform silica shells of controlled thickness. We suggest that this method

(56) Pérez-Juste, J.; Pastoriza-Santos, I.; Liz-Marzán, L. M.; Mulvaney, P. *Coord. Chem. Rev.* **2005**, *249*, 1870.

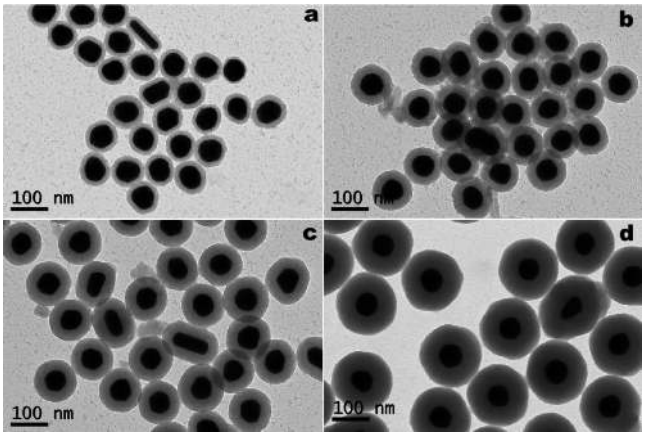

Figure 4. TEM images of 60.4 nm Au spherical particles coated with different silica shell thicknesses: (a) 11.7 ± 1.5, (b) 22.4 ± 2.3, (c) 28.7 ± 1.5, and (d) 43.7 ± 3.5 nm.

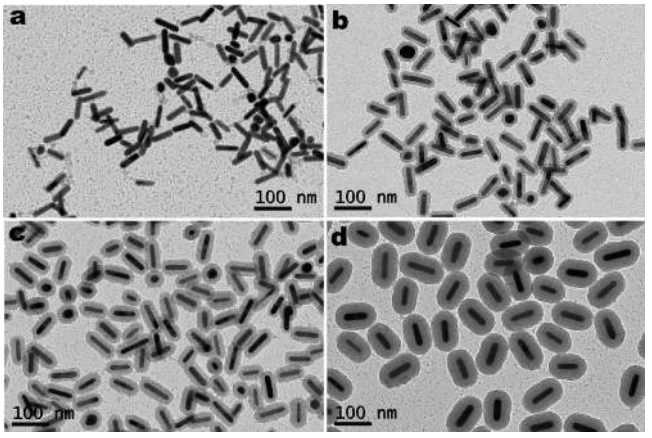

Figure 5. TEM images of Au nanorods (67.4 nm long, 14.3 nm thick) coated with silica shells of different thicknesses: (a) 3.7 ± 0.5, (b) 9.1 ± 1.6, (c) 18.9 ± 1.6, and (d) 30.7 ± 2.5 nm.

might be readily extended to any PEG-coated colloid. In what follows, we demonstrate that these Au@SiO_2 systems are suitable candidates as surface-enhanced resonance Raman scattering (SERRS) encoded particles for their use in biolabeling, medical imaging, multiplexed high-throughput screening, and labeling of commercial goods, documents, and bank notes. In this kind of composite particles, silver or gold cores provide a high electromagnetic field (when their corresponding plasmon resonance modes are excited) necessary to enhance the Raman signal of a given SERS/SERRS reporter whereas the silica shell not only protects the Raman tag from leaching but also inhibits the adsorption of other molecular systems onto the metallic surfaces, which might interfere with the vibrational code. The silica shell additionally provides the suspensions with high colloidal stability as well as an ideal surface for covalent functionalization (of biomolecules, for example). A demonstration of this capability was carried out with 60 nm gold spheres as SERRS substrates and three different blue dyes to envisage the multiplexing capability. Figure 6a shows the absorption and emission spectra of the three cationic dyes used as Raman probes: Nile blue A (NBA), toluidine blue O (TB), and methylene blue (MB). Encapsulation of the dyes was carried out by simply adding the dye (dissolved in ethanol) to the PEG-stabilized Au colloids immediately before TEOS addition. The cationic nature of the dyes was likely to drive adsorption during silica coating, and no effect was observed on either particle

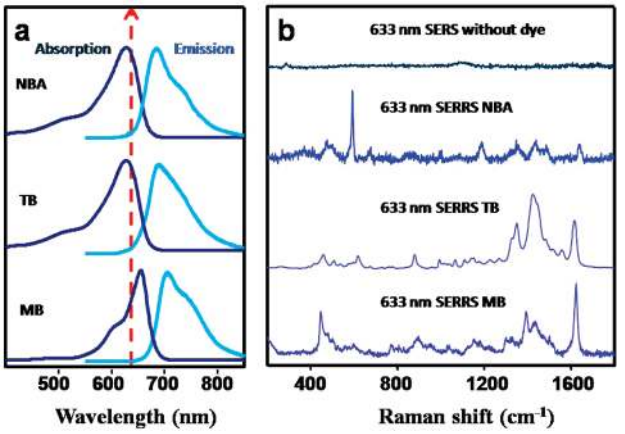

Figure 6. (a) Absorption and emission spectra of Nile blue A (NBA), toluidine blue O (TB), and methylene blue (MB). (b) SERRS spectra of Au@SiO_2, both unlabeled and labeled with NBA, TB, and MB. All spectra were obtained upon excitation with a 633 nm laser (indicated with a red arrow in plot a).

stability or silica shell quality, as revealed by TEM images and vis−NIR spectra in Figure S3. TEM showed that each individual Au nanoparticle was coated with a thin, uniform silica shell of around 25 nm for NBA and MB and 18 nm for TB, and the spectra in solution displayed the expected SPB red shift.

The optical-enhancing activity of the Au@SiO_2 nanoparticles is demonstrated in Figure 6b, where we plotted the SERRS spectra obtained upon excitation with a 633 nm laser line in resonance with the electronic absorption bands of all three dyes (Figure 6a). Although no signal was observed from the unlabeled Au@SiO_2, the characteristic enhanced signals were recorded from the labeled beads: ring stretching (1643, 1492, 1440, 1387, 1351, and 1325 cm^{-1}), CH bending (1258 and 1185 cm^{-1}), and in-plane CCC and NCC (673 cm^{-1}), CCC and CNC (595 cm^{-1}), and CCC (499 cm^{-1}) deformations for NBA;[57] ring stretching (1616, 1559, and 1444 cm^{-1}), CH bending (1424, 1109, and 1064 cm^{-1}), and in-plane CCC and CNC (1350, 1330, 994 cm^{-1}) and CCC and CSC (508 and 459 cm^{-1}) deformations for TB;[58] and ring stretching (1624 and 1503 cm^{-1}), CH bending (1392 and 1038 cm^{-1}), and in-plane CCC and CNC (1435, 1152, 481, and 447 cm^{-1}) deformations for MB.[59] Notably, none of the dyes showed more than residual fluorescence, indicating, together with the SERRS spectra, that the molecular probes were chemisorbed onto the gold surfaces and thus fluorescence was quenched. The diversity of possible SERS/SERRS reporters that can be incorporated within these coated particles hints at their multiplexing potential.

Conclusions

We have demonstrated the advantages of using poly(ethylene glycol) as a primer for silica coating gold nanoparticles. Upon the replacement of other capping agents necessary for their synthesis, gold nanoparticles of different sizes and shapes can be transferred into ethanol, where silica can be directly grown through the standard Stöber process. Apart from the generality with respect to particle size and shape, uniform, homogeneous silica coatings are obtained with fine control over shell thickness. We have additionally presented a proof of concept for the use of this

(57) Alvarez-Puebla, R. A.; Contreras-Cáceres, R.; Pastoriza-Santos, I.; Pérez-Juste, J.; Liz-Marzán, L. M. *Angew. Chem., Int. Ed.* **2009**, *48*, 138.
(58) Mazeikiene, R.; Niaura, G.; Eicher-Lorka, O.; Malinauskas, A. *Vib. Spectrosc.* **2008**, *47*, 105.
(59) Xiao, G. N.; Qing Man, S. Q. *Chem. Phys. Lett.* **2007**, *447*, 305.

method to fabricate SERS/SERRS-encoded nanoparticles via the incorporation of Raman-active molecules during silica growth. This can be readily carried out with a variety of dyes and nonresonant molecules, which will facilitate multiplexed biolabeling.

Acknowledgment. I.P.-S. acknowledges the Isidro Parga Pondal Program (Xunta de Galicia, Spain) and R.A.A.-P. and J.P.-J. acknowledge the Ramón y Cajal Program (MEC, Spain). This work has been funded by the Spanish Ministerio de Educación y Ciencia (Consolider Ingenio NANOBIOMED, MAT2007-62696 and MAT2008-05755), Xunta de Galicia (PGIDIT06TMT31402PR and 08TMT008314PR), and the EU (NANODIRECT, grant number CP-FP 213948-2).

Supporting Information Available: Vis−NIR absorbance spectra of CTAB-stabilized Au spherical nanoparticles dispersed in water and transferred into ethanol through mPEG-SH modification. TEM images of Au spherical particles coated with homogeneous silica shells. Vis−NIR absorbance spectra of Au@PEG and Au@SiO_2 dispersions in ethanol and TEM images of the corresponding Au@SiO_2 particles. This material is available free of charge via the Internet at http://pubs.acs.org.